

A casualty of climate change? Loss of freshwater forest islands on Florida's Gulf Coast

Amy K. Langston¹ | David A. Kaplan¹  | Francis E. Putz²

¹Engineering School of Sustainable Infrastructure and Environment, University of Florida, Gainesville, FL, USA

²Department of Biology, University of Florida, Gainesville, FL, USA

Correspondence

David A. Kaplan, Engineering School of Sustainable Infrastructure and Environment, University of Florida, Gainesville, FL, USA.
Email: dkaplan@ufl.edu

Abstract

Sea level rise elicits short- and long-term changes in coastal plant communities by altering the physical conditions that affect ecosystem processes and species distributions. While the effects of sea level rise on salt marshes and mangroves are well studied, we focus on its effects on coastal islands of freshwater forest in Florida's Big Bend region, extending a dataset initiated in 1992. In 2014–2015, we evaluated tree survival, regeneration, and understory composition in 13 previously established plots located along a tidal creek; 10 plots are on forest islands surrounded by salt marsh, and three are in continuous forest. Earlier studies found that salt stress from increased tidal flooding prevented tree regeneration in frequently flooded forest islands. Between 1992 and 2014, tidal flooding of forest islands increased by 22%–117%, corresponding with declines in tree species richness, regeneration, and survival of the dominant tree species, *Sabal palmetto* (cabbage palm) and *Juniperus virginiana* (southern red cedar). Rates of *S. palmetto* and *J. virginiana* mortality increased nonlinearly over time on the six most frequently flooded islands, while salt marsh herbs and shrubs replaced forest understory vegetation along a tidal flooding gradient. Frequencies of tidal flooding, rates of tree mortality, and understory composition in continuous forest stands remained relatively stable, but tree regeneration substantially declined. Long-term trends identified in this study demonstrate the effect of sea level rise on spatial and temporal community reassembly trajectories that are dynamically re-shaping the unique coastal landscape of the Big Bend.

KEYWORDS

cabbage palm, coastal forest, community reassembly, *Sabal palmetto*, sea level rise, tidal flooding, vegetation shift

1 | INTRODUCTION

As chronicled in an ever-growing body of research, climate change is driving spatial and compositional shifts in vegetation at local, regional, and global scales (e.g., Kelly & Goulden, 2008; Leffler, Klein, Oberbauer, & Welker, 2016; Svenning & Sandel, 2013; Walther et al., 2002). In coastal areas, sea level rise, warming air temperatures, and changing rainfall regimes elicit short- and long-term changes in vegetation by altering physical conditions that affect the survival, distribution, and reproductive success of

coastal plants (Gabler et al., 2017; Kirwan, Guntenspergen, & Morris, 2009; Liu, Conner, Song, & Jayakaran, 2017; Osland et al., 2016; Scavia et al., 2002). The maintenance of salt marsh, for example, largely depends on feedbacks among sediment availability, plant productivity, and the local rate of sea level rise (e.g., Craft et al., 2009; Fagherazzi et al., 2012; Kirwan & Megonigal, 2013; Reed, 1995). Increases in hurricane intensity resulting from increases in sea surface temperature are expected to produce larger storm surges with concomitant increases in the frequency of damage from scour, erosion, vegetation burial, and saltwater

intrusion (Lin, Emanuel, Oppenheimer, & Vanmarcke, 2012; Mendelsohn, Emanuel, Chonabayashi, & Bakkensen, 2012; Michener, Blood, Bildstein, Brinson, & Gardner, 1997). Droughts, particularly in concert with sea level rise, also affect coastal vegetation by increasing salt concentrations in drying soil beyond specific tolerance levels (Angelini & Silliman, 2012; Cormier, Krauss, & Conner, 2013; White & Kaplan, 2017; Williams, MacDonald, & Sternberg, 2003).

Coastal plants have adapted to survive periodic disturbances, but it is unclear how they will fare in a future with more frequent or severe pulse events coupled with chronic changes in sea level and temperature (Leonardi, Ganju, & Fagherazzi, 2016; Michener et al., 1997). To improve our understanding, we can investigate responses of coastal plants along coastlines largely undisturbed by land-use changes that exacerbate the effects of climate change. Of particular value are long-term field data that capture transitions in coastal vegetation communities.

The Big Bend coast of Florida is a relatively undisturbed, sparsely developed area that is ideal for studying long-term trends in coastal ecosystems. This 250-km stretch of coastline extends along the Gulf of Mexico from Apalachee Bay south to Anclote Key (Mattson, Frazer, Hale, Blitch, & Ahijevych, 2007). Hydrology along the Big Bend is driven by a combination of saltwater and freshwater sources. The Gulf of Mexico and an extensive network of tidal creeks deliver saltwater while freshwater is supplied by precipitation [127–152 cm annually (FCC, 2014)], springs from the Floridan aquifer, and several major rivers. The region is subjected to little subsidence due to the presence of a stable carbonate platform and experiences low wave energy (tidal range of approximately 1 m), but its low elevation and shallow topographic relief mean that small increases in sea level affect large areas (DeSantis, Bhotika, Williams, & Putz, 2007; Raabe, Streck, & Stumpf, 2004; Raabe & Stumpf, 2016; Williams, MacDonald, McPherson, & Mirti, 2007; Williams, Pinzon, Stumpf, & Raabe, 1999). Based on the tide station in Cedar Key, Florida, mean sea level increased along the Big Bend coast by an average of 1.93 mm/year between 1914 and 2014 (NOAA, 2013). While local mean sea level is rising at a lower rate than in other coastal regions of Florida, changes in air temperature, barometric pressure, and ocean circulation have created variability in the rate of local sea level change within this time period, including short-term, rapid increases much greater than 1.93 mm/year. These short-term increases may have greater effects on coastal plants than long-term mean sea level rise, as they occur on timescales similar to the turnover times of plant communities.

Storms and droughts have played important roles in shaping the Big Bend and altering vegetation communities. Recent major events include an extratropical storm in 1993, dubbed the “Storm of the Century,” which caused high tree mortality in stands of coastal forest and deposited sediment equivalent to 10 years of averaged accretion in Gulf Coast marshes (Goodbred & Hine, 1995). Following the 1993 storm, a 5-year drought (1998–2002), one of the worst in

Florida’s history, resulted in record low freshwater flows along the Big Bend and also contributed to tree mortality (Verdi, Tomlinson, & Marella, 2006; Williams et al., 2003).

Historically, the Big Bend has been subject to high rates of vegetation community reassembly, making it a useful region for examining the effects of climate change on coastal vegetation. Historical changes in shoreline and intertidal habitats reported by a U.S. Geologic Survey show major transitions from upland forest to marsh and marsh to open water from 1852 to 1995 (Raabe et al., 2004). The Big Bend supports a diversity of coastal communities, including extensive salt marsh, coastal forest (bottomland hardwood swamp, slash pine flatwood woodlands, cypress-tupelo swamp forest, coastal hydric hammock, and tidal freshwater forest), scattered stands of mangrove, and seagrass beds. Characteristic of the region are islands of freshwater forest (hereafter, forest islands), which are isolated remnants of a formerly continuous forest that is retreating landward (DeSantis et al., 2007; Geselbracht, Freeman, Kelly, Gordon, & Putz, 2011; Kurz & Wagner, 1957; Williams, Ewel, Stumpf, Putz, & Workman, 1999; Williams, MacDonald, et al., 2007; Williams, Pinzon, et al., 1999). These islands are the focus of our study.

Forest islands, which are dominated by *Sabal palmetto* (cabbage palm) and *Juniperus virginiana* (southern red cedar) occur on elevated limestone substrate surrounded by salt marsh. Limestone rock is often exposed or near the surface and regional karst topography creates a dimpled surface with variable soil depths, affecting water storage potential across islands. Unlike continuous coastal forests that obtain freshwater from both direct precipitation and the Floridan aquifer, trees on forest islands are primarily dependent on precipitation (DeSantis et al., 2007; Williams, MacDonald, et al., 2007). Other trees common on healthy islands include *Quercus virginiana* (live oak), *Celtis laevigata* (sugarberry), and *Persea palustris* (swamp bay). Although considered a freshwater forest, tree species vary in their salt tolerances. More tolerant species are able to persist in more tidally inundated islands while others disappear (Williams, Meads, & Sauerbrey, 1998). *Sabal palmetto*, one of the most salt-tolerant trees in the southeastern United States (Perry & Williams, 1996), is the sole tree species on the most saline islands.

Presented here are the most recent findings of a long-term field study of freshwater forest response to climate change drivers along a tidal creek, with new insight on community reassembly trajectories occurring in forest islands. Our findings are representative of vegetation change observed across the Big Bend, where the landscape is shifting from a mosaic of freshwater and saltwater communities to one composed exclusively of halophytic vegetation, particularly in regions lacking major freshwater inputs (i.e., far from major rivers). We hypothesized that contemporary declines of forest islands follow long-term trends and that the trajectory of community reassembly in remnant forest islands varies with elevation and tidal flooding frequency. To address these hypotheses, we compare changes in tidal flooding and weather to long-term trends in tree mortality, regeneration, and understory vegetation in remnant forest islands.

2 | MATERIALS AND METHODS

2.1 | Study site

The study site is located along Turtle Creek, a tidal creek in Florida's Waccasassa Bay Preserve State Park (29°7'N, 82°47'W; Figure 1) approximately 5 km from the Waccasassa River, which is the nearest major surface freshwater source (mean annual discharge = 6.97 m³/s; USGS, 2012). Plant communities at the study site include salt marsh dominated by *Juncus roemerianus* (black needle rush) and forest islands that transition to continuous coastal freshwater forest and pine flatwoods inland. Turtle Creek is the setting of several previous studies on forest retreat (Castaneda & Putz, 2007; DeSantis et al., 2007; Geselbracht et al., 2011; Perry & Williams, 1996; Williams et al., 1998, 2003; Williams, Ewel, et al., 1999), all of which used data from 13 permanent sample plots established in 1992 and 1993. Of the 13 plots, 10 occur on forest islands in various states of decline: four were initially identified as "healthy" (H0, H1, H2, H3), three as "intermediate" (I1, I2, I3), and three as "decadent" (D1, D2, D3) when the study commenced. The remaining three plots are in continuous forest (C1, C2, C3) and, along with H0, were established

in 1993. Each plot is 400 m², and all but one is 20 × 20 m (D1 is 40 × 10 m due to the narrow shape of the island).

2.2 | Tidal flooding frequency, ground elevation, and soil depth

To evaluate the influence of tidal flooding on vegetation, we analyzed tidal and elevation datasets for the study plots and compared them to historical and recent field data. Weekly tidal flooding measurements were collected in nine of the 13 plots from May 1992 to January 1993 (Williams, Ewel, et al., 1999). Plots C1–C3 and H0 were established after the tidal flooding study; these plots were assumed to flood no more frequently than plot H1. Using field data, Williams, Ewel, et al. (1999) developed a tidal flooding model to calculate tidal flooding frequencies in other years. Tidal flooding frequency was defined as the number of weeks during which flooding occurred at least once and was predicted using median plot elevation, mean higher high water (MHHW) for a specified time period as recorded in Cedar Key, FL (National Oceanic and Atmospheric Administration [NOAA] Station 8727520), and plot distance from the mouth of Turtle Creek. We used this same model to estimate weeks



FIGURE 1 Study site at (a) Turtle Creek on (b) the Big Bend coast in Florida; Turtle Creek is marked with a star. Island plots are labeled by their condition in 1992 and 1993: H = healthy (light gray); I = intermediate (dark gray); D = decadent (black). C plots occur in continuous coastal forest (white)

of tidal flooding in 2014 (i.e., during the time of our most recent tree census) and 1994 (during which understory vegetation data were previously collected). The model was not applied to the three continuous forest plots or the two higher elevation healthy island plots (H0 and H1) because Williams, Ewel, et al. (1999) found the model described tidal flooding well only in the eight lower elevation island plots.

We compared 1992–1993 elevation data reported in Williams, Ewel, et al. (1999) to 2007 LiDAR (Light Detection and Ranging) data from the Florida Division of Emergency Management (FDEM) for Levy County, downloaded from the NOAA Digital Coast website (coast.noaa.gov/digitalcoast/). Raster data and shapefiles of plot boundaries were viewed in ArcGIS (v. 10.1; Esri, Redlands, CA, USA). All data layers were in horizontal coordinate system WGS84 and the vertical spatial reference for the raster file was NAVD88 (altitude resolution of 0.0328 ft.). We sampled 25 pixels within each plot in a 5 × 5 m grid pattern, mimicking laser-level survey sampling reported by Williams, Ewel, et al. (1999). The sampling pattern was repeated three times for a total of 75 sampled pixels per plot (with the exceptions of H2, C1, and C2, for which fewer pixels were sampled because raster data were incomplete). Vertical pixel values were converted to meters and compared to elevation data reported in table 1 of Williams, Ewel, et al. (1999).

Soil depth to limestone was measured at ten random locations within the original nine island plots between fall 2015 and spring 2016 by inserting a pin flag into the soil until it hit rock, then measuring the inserted length with a metric ruler. We used the Kruskal–Wallis test to compare soil depths between plot types, and multiple regression to evaluate whether soil depth depended on elevation and flooding frequency. All statistical analysis, unless otherwise stated, was performed in R (R Core Team, 2016).

2.3 | Precipitation, climate, and storms

We reviewed meteorological (precipitation and temperature) and storm data from 1955 to 2014 for the Big Bend coast to identify extreme weather events that occurred since the last tree census (2005) that may correlate with vegetation trends as well as to identify long-term climate patterns. Annual climatological summary data were obtained from NOAA: National Centers for Environmental Information (NCEI) for the Tampa International Airport weather station (#12842), which is approximately 140 km southeast of the study site and the nearest station with continuous historical temperature and precipitation records. Storm data for Levy County from 1955 to 2014 were obtained from NOAA NCEI Storm Events Database and were compared to NOAA National Hurricane Center historical summaries and NOAA Storm Predictor Center maps. La Niña events recorded by NOAA National Weather Service Climate Prediction Center were reviewed to identify droughts that occurred since 2005. Waccasassa River discharge data from 1963 to 2014 (USGS gage #02313700) were also reviewed as an integrated measure of regional-scale precipitation and temperature variability. Annual discharge data were summarized by calculating cumulative deviation

from mean annual discharge. Years with above-average flow were given a value of +1 and years with below-average flow were assigned a value of −1. Long-term trends were assessed by summing cumulative wet and dry trends across the period of record.

2.4 | Tree demography data

To test the hypothesis that contemporary declines of forest islands follow long-term trends, we censused trees in all 13 plots in summer 2014. Censuses (complete and partial) were previously conducted annually from 1992 to 1998, and in 2000 and 2005. During the 2014 census and previous censuses, tree species and status (live/dead) were recorded for each tree >2 m tall, with the exception of *S. palmetto*, for which census data were recorded for trees with above-ground trunks of any height. In summer 2015, we measured tree regeneration by counting all *S. palmetto* without visible trunks (“trunkless”) and all other trees <2 m tall, including small seedlings, in each plot.

We used a nonlinear least squares logistic model to evaluate relationships between 2014 vegetation data and tidal flooding frequency for all 13 plots. Correlation between tree death and salt marsh vegetation in 2014 was examined using simple linear regression. We compared tree regeneration of all species previously reported for 2005 in table 1 of DeSantis et al. (2007) and compared 2014/15 census results [tree species richness, *S. palmetto* regeneration, and *S. palmetto* density (of trees with trunks)] to 1992/93 census results (1992 data were used for all island plots except H0, and 1993 data were used for continuous forest plots and H0). 2014 *S. palmetto* regeneration data were compared to 1992/1993 regeneration by compiling trunkless *S. palmetto* counts reported in table 1 of Williams, Ewel, et al. (1999) and seedling counts estimated from figure 5a in the same paper. Comparisons of tree species richness and *S. palmetto* regeneration were made using Wilcoxon signed rank tests. Densities of *S. palmetto* with trunks were compared using paired *t* tests. To evaluate trends in tree survival during the census period (1992–2014), we calculated annual mortality rates for *S. palmetto* and *J. virginiana* by plot type (continuous, healthy, intermediate, and decadent) using the mortality equation developed by Sheil, Burslem, and Alder (1995). We fitted tree mortality in continuous and healthy plots with a simple linear model and intermediate and decadent plots with a nonlinear least squares logistic model to describe mortality trends.

2.5 | Understory composition

We conducted an understory survey in the fall and winter of 2014/2015 to test our hypothesis that community reassembly in forest islands varies with tidal flooding frequency. Plots were surveyed during three field visits, and understory species were surveyed using the same sampling grid of 25 1 m² random subplots per 400 m² study plot used in 1994, the only other time when understory vegetation was previously assessed. Subplots were located along five transects across each plot, and the same subplot grid was used for

all 20 × 20 m plots. A separate sampling grid was created for D1 (40 × 10 m). Within each subplot, absolute percent cover of each nontree species was recorded. A sample of each species was collected and pressed for reference, and those species that could not be identified in the field were later identified using floras, keys, the Waccasassa floristic survey (Abbott & Judd, 2000), and the species list in the Appendix of Williams, Ewel, et al. (1999). We compared overall species richness in 2014 to the 1994 understory composition (raw data provided by K. Williams) using a paired *t* test. We evaluated community reassembly patterns across tidal flooding frequencies between 1994 and 2014, and connected data points using a loess smooth function.

We compared understory composition in 1994 and 2014 with nonmetric multidimensional scaling (NMS) in PC-ORD (MJM Software Design, Gleneden Beach, OR, USA). Understory data in 1994 were recorded as number of subplots per plot in which each plant species occurred, which we assumed to be comparable to percent cover. We ran the NMS procedure for each dataset five times, each time with a new random seed, to verify consistency of our interpretation among the solutions, as recommended by Peck (2010). Convex hulls were used to outline ordination spaces of plots according to categorized tidal flooding frequencies (0–1 week, 2–9 weeks, 10–19 weeks, 20–29 weeks, and >30 weeks).

3 | RESULTS

3.1 | Tidal flooding frequency, ground elevation, and soil depth

Tidal flooding frequency increased dramatically between 1992 and 2014 in the eight lowest elevation island plots (Table 1). The number of weeks in which tidal flooding of island plots occurred ranged from 0–27 in 1992 and 0–33 in 2014, but increased by approximately 6 weeks in each of the eight lowest elevation island plots. For healthy island plots H2 and H3, this corresponded to 117% and 86% increases in flooding frequency, respectively, within 22 years. Flooding frequencies of intermediate island plots (I1–I3) increased to 18–20 weeks (an average increase of 45%), and flooding in decadent plots increased to 24–33 weeks (an average increase of 26%) in 2014. In the two most frequently flooded plots (D2 and D3), tidal flooding events occurred during approximately 50% of weeks in 2014. Continuous forest plots and H0 were previously assumed to flood no more than H1, which flooded during 1 week in 1992. Continuous forest plots are inland enough that correlation between tidal flooding and elevation is weak, and we found no evidence of flooding in those plots or in H0 and H1 during repeated field visits in 2014, but we know that H1 is flooded during major storms. As such, we assumed flooding frequency in the continuous forest plots and H0 and H1 had not changed since 1992.

Median elevations derived from LiDAR data were mostly within 0.02 to 0.08 m of those from the original field data (Table 1). The largest difference was in plot H2 (median LiDAR elevation was 0.15 m higher than median field elevation), likely due to

TABLE 1 Summary of elevations and tidal flooding frequencies in the study plots between 1992 and 2014

Plot	Median elevation (m NAVD88)		Tidal flooding frequency (weeks) ^c		
	Original ^a	LiDAR ^b	1992	1994	2014
C1	1.10	1.18	0	0	0
C2	1.09	1.06	0	0	0
C3	0.69	0.60	0	0	0
H0	0.96	1.01	0	0	0
H1	0.93	0.91	1	1	1
H2	0.78	0.93	6	6	13
H3	0.80	0.87	7	6	13
I1	0.60	0.68	14	13	20
I2	0.67	0.75	14	14	20
I3	0.66	0.78	12	11	18
D1	0.52	0.56	18	17	24
D2	0.58	0.62	26	25	32
D3	0.63	0.68	27	27	33

^aFrom table 1 in Williams, Ewel, et al. (1999); elevations measured in the 1990s with a laser transit, 25 estimates per plot.

^bCalculated from 2007 LiDAR data from FDEM for Levy County, FL.

^cFlooding frequencies based on calendar year; flooding in H2, H3, I plots, and D plots calculated using model by Williams, Ewel, et al. (1999); flooding in C plots, H0, and H1 assumed to be the same as in 1992. Values for 1992 differ from those reported in Williams, Ewel, et al. (1999) because they were originally based on a 37-week study.

approximately 25% of pixels in the LiDAR raster file missing within the plot boundary, resulting in fewer sampled pixels. Elevation ranges from LiDAR data for all island plots were slightly higher than but completely overlapped with the original elevation ranges. Because field measurements were so precisely measured by Williams, Ewel, et al. (1999), and little difference was found between the original measurements and median LiDAR data, we accepted the field measurements as the most accurate elevations for the study plots and used those values in the tidal flooding model and soil depth analysis.

Mean soil sample depths varied widely across the original nine island plots (2.54–30.23 cm; Figure 2). We found no differences in soil depths between islands in different states of decline (Kruskal–Wallis $\chi^2 = 1.00$, $p = .61$; based on median soil depth), although soil depth differed between intermediate plots ($K-W = 17.82$, $p = .0001$) and between decadent plots ($K-W = 18.96$, $p < .0001$). Within plot variation was similar among decadent plots, relatively high in I2 and I3, and increased with elevation among healthy plots. Neither median elevation nor tidal flooding frequency explained soil depth across island plots ($F_{2,6} = 0.86$, $p = .47$), due to high variation within plots and outlier soil depths in I2.

3.2 | Precipitation, climate, and storms

Precipitation during 2005–2014 was within the 1955–2005 range (Figure 3a), a period of record previously evaluated by DeSantis et al.

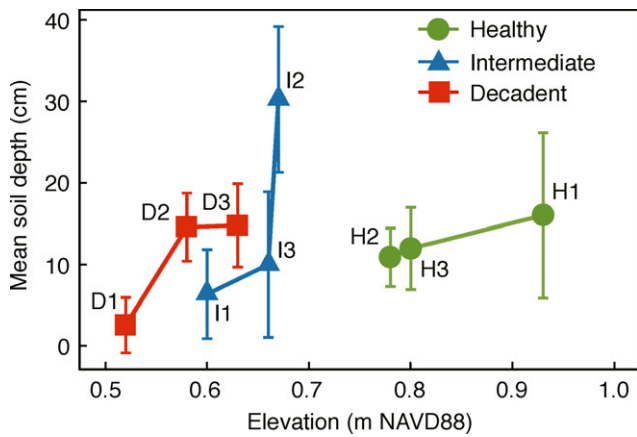


FIGURE 2 Mean soil depth with standard deviation error bars across elevation for the original nine island plots (labeled). Soil depths are grouped by island condition as defined in 1992. Elevation data are from Williams, Ewel, et al. (1999)

(2007). The 59-year annual mean (1955–2014) was 118 cm, compared to the 50-year annual mean (1955–2005) of 117 cm. For the period 2005–2014, we identified no unusual rain years, nor did we identify any anomalies in air temperature extremes. Very slight increases in mean annual, maximum, and minimum temperatures are evident since 1955 but rates did not approach the current rate of global annual temperature increase of 0.07°C (NOAA, 2016). Three La Niña events, defined by NOAA as ocean temperatures deviating by at least -0.5°C from the mean sea surface temperature of a 30-year base period (NOAA, 2015), occurred since 2005 (July 2007–July 2008, June 2010–May 2011, and July 2011–April 2012). Two La Niña events (2007–2008 and 2010–2011) corresponded to years that experienced negative deviations from the 59-year mean annual rainfall, but were far smaller than the negative deviations that occurred during the major

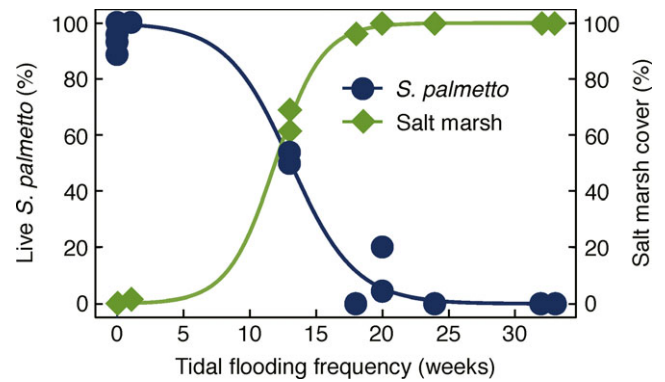


FIGURE 4 Percent of live *Sabal palmetto* of total *S. palmetto* present per plot in 2014 and percent salt marsh understory cover across a tidal flooding frequency gradient. Data are fitted with nonlinear logistic growth/decay models

1998–2002 drought. Cumulative deviations from mean annual discharge from the Waccasassa River show that while annual discharge varied, flow declined overall since at least 1999 (and possible since 1989, though data for 1993–1998 are incomplete; Figure 3b), which is the longest period of reduced flow in the 1963–2014 record.

The 1993 “Storm of the Century” and a 5-year drought (1998–2002) were previously identified as contributing to periods with increased rates of tree mortality in the original nine island plots (DeSantis et al., 2007; Williams et al., 2003). We identified 1 year in our review of meteorological and storm data in which more recent extreme weather events occurred that could have affected the study site. In 2012, Hurricane Beryl produced a small (EF-0) tornado in Yankeetown, FL, approximately 11 km south of the study site, and a 1.4-m storm surge was documented 1 month later in Cedar Key from Hurricane Debby (Kimberlain, 2012).

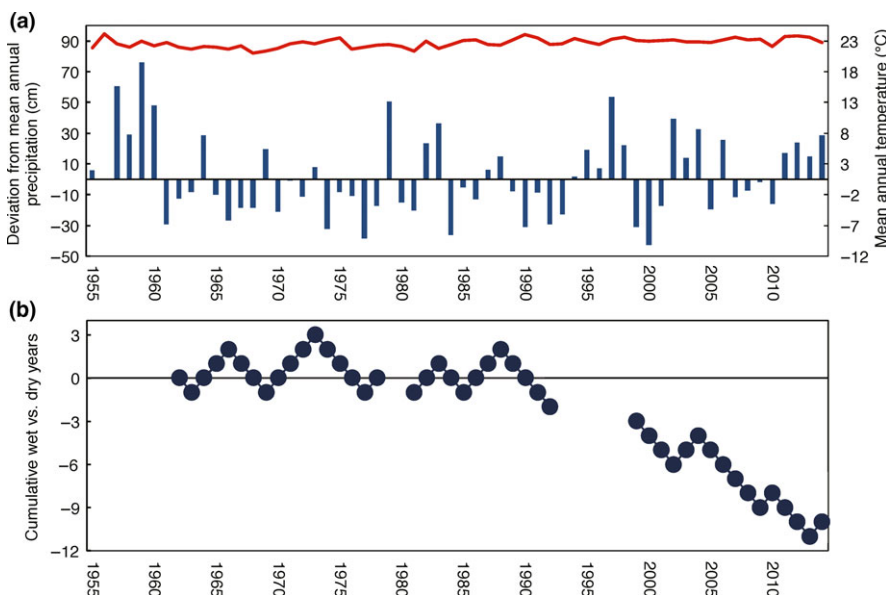


FIGURE 3 Trends in (a) mean annual temperature (line) and deviations from mean annual precipitation (bars) from 1955 to 2014, and (b) running total of cumulative years above and below long-term mean annual discharge (horizontal line at 0) from Waccasassa River from 1963 to 2014, excluding years for which little or no data are available

TABLE 2 Regeneration status of tree species in 2014 relative to 2005 across plots, arranged from lowest to highest flooding frequency

Plot	C1	C2	C3	H0	H1	H2	H3	I3	I1	I2	D1	D2	D3
Flooding frequency (weeks)	0	0	0	0	1	13	13	18	20	20	24	32	33
<i>Sabal palmetto</i> (cabbage palm)	R	R	R	R	R	[X]	[X]	L	X	X	L	L	–
<i>Juniperus virginiana</i> (southern red cedar)	R	R	R	R	R	X	L	L	L	–	–	–	–
<i>Quercus virginiana</i> (live oak)	X	R	[X]	X	R	L	L	–	–	–	–	–	–
<i>Quercus laurifolia</i> (laurel oak)	–	L	[X]	L	–	–	–	–	–	–	–	–	–
<i>Celtis laevigata</i> (sugarberry)	X	[X]	X	–	X	–	X	–	–	–	–	–	–
<i>Morus rubra</i> (red mulberry)	–	–	L	–	L	–	–	–	–	–	–	–	–
<i>Pinus taeda</i> (loblolly pine)	[X]	–	L	–	–	–	–	–	–	–	–	–	–
<i>Diospyros virginiana</i> (persimmon)	L	–	[X]	–	–	–	–	–	–	–	–	–	–
<i>Ulmus alata</i> (winged elm)	–	–	L	–	–	–	–	–	–	–	–	–	–
<i>Ptelea trifoliata</i> (hoptree)	–	L	–	–	–	–	–	–	–	–	–	–	–
<i>Fraxinus caroliniana</i> (Carolina ash)	–	L	–	–	–	–	–	–	–	–	–	–	–
<i>Acer floridanum</i> (Florida maple)	–	X	–	–	–	–	–	–	–	–	–	–	–
<i>Gleditsia tricanthos</i> (honey locust)	–	–	X	–	–	–	–	–	–	–	–	–	–
<i>Persea borbonia</i> (red bay)	R	–	–	–	–	–	–	–	–	–	–	–	–

Following the same nomenclature as DeSantis et al. (2007), tree species are categorized as currently regenerating (R), relict stands (X), converted from regenerating to relict stands between 2005 and 2014 [X], observed in 2005 but absent in 2014 (L), and not present in 2005 but found to be regenerating in 2014 (R). Categories (L) and (R) were not used in DeSantis et al. (2007).

3.3 | Tree census and 2014 vegetation trends

We found a strong relationship between 2014 *S. palmetto* mortality and tidal flooding frequency (Figure 4). In continuous forest plots and H0 and H1, which never or rarely flood, live *S. palmetto* (with trunks) relative to total *S. palmetto* (live and dead) per plot ranged from 89% to 100%. In the other two healthy island plots, where tidal flooding occurred during approximately 13 weeks of 2014, only 50%–54% of the trees were alive. Among the remaining six island stands in which flooding frequency ranged from 18 to 33 weeks, only two intermediate plots had any live *S. palmetto* in 2014. Both plots had one live tree each. The trend in *S. palmetto* survival across tidal flooding frequency was best described by a nonlinear least squares logistic model, which explained 98% of the variance between *S. palmetto* survival and tidal flooding frequency. We found a similarly strong but opposite trend between 2014 salt marsh species cover and tidal flooding frequency ($R^2 = 0.99$; Figure 4). Tree death was positively correlated with increased salt marsh cover across the 13 plots ($r^2 = 0.96$; $F_{(1,11)} = 256.8$, $p < .0001$). No salt marsh vegetation was present in the continuous forest plots or H0 and only 1% was found in H1. The proportion of salt marsh vegetation in the other two healthy island stands ranged from 61% to 69%, and the understories of intermediate and decadent plots were composed of 96%–100% salt marsh species.

Fewer regenerating tree species were found in 2014 compared to 2005 in both continuous forest and island plots (Table 2). In continuous forest stands, regeneration of *Quercus laurifolia* (laurel oak), *C. laevigata*, *Pinus taeda* (loblolly pine), and *Diospyros virginiana* (persimmon) ceased by 2014 and regenerating *Q. virginiana* persisted only in C2. Small *Persea borbonia* (red bay; <2 m tall), which were

absent in 2005, were found in C1 in 2014. *Sabal palmetto* and *J. virginiana* were still regenerating in continuous forest plots and in H0 and H1 in 2014. H1 was the only island plot with regenerating *Q. virginiana* in 2014. Tree regeneration ceased in all other island plots; *S. palmetto* in H2 and H3 converted to relict (nonregenerating) stands between 2005 and 2014.

The 2014 tree census revealed continued forest decline with increased tidal flooding on island plots as measured by species richness, *S. palmetto* regeneration, and *S. palmetto* density (Figure 5). Declines were pronounced with respect to species richness ($V = 78$, $p = .002$; Figure 5a) and *S. palmetto* regeneration ($V = 55$, $p = .006$; Figure 5b) between 1992/93 and 2014. Trunkless *S. palmetto* density was reduced by 85%–93% by 2014 in continuous forest plots, and by 79%–87% in H0 and H1. Smaller differences were found in intermediate and decadent stands, where lower elevations and greater susceptibility to tidal flooding and storm surges had already limited regeneration in 1992/93. Density of *S. palmetto* with trunks was also much reduced between 1992/93 and 2014 ($t = 4.45$, $p = .0001$; Figure 5c). *Sabal palmetto* density was much higher in healthy and intermediate islands subject to more than 1 week of tidal flooding in 1992, whereas density remained similar in continuous forest and H0 and H1 between 1993 and 2014.

Looking across the >20-year period of record for plots along Turtle Creek, rates of tree mortality of the dominant tree species remained near zero in continuous forest and healthy island plots (Figure 6a,b), but increased very rapidly in intermediate and decadent island plots (Figure 6c,d). Mortality of *J. virginiana* increased rapidly and nonlinearly in intermediate and decadent plots over time, as demonstrated with well-fitted logistic curves ($R^2 = 0.97$ for

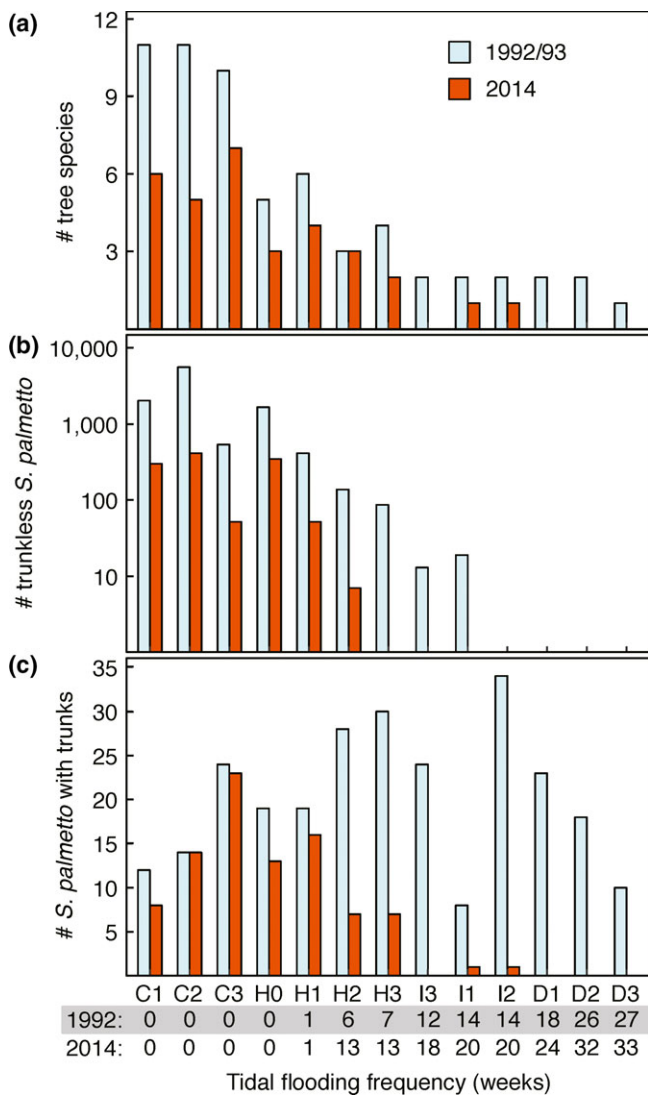


FIGURE 5 Comparison of 1992/1993 and 2014 census data showing declines in (a) tree species richness, (b) number of trunkless *Sabal palmetto* (counts are shown on a log scale), and (c) number of live *S. palmetto* with trunks for each plot, arranged in order from low to high tidal flooding frequencies in 1992 and 2014

intermediate plots; $R^2 = 0.84$ for decadent plots). Nonlinear trends of *S. palmetto* mortality in intermediate and decadent plots were also very well described by logistic curves ($R^2 = 0.88$, $R^2 = 0.98$, respectively). In intermediate plots, the rate of *J. virginiana* mortality increased faster than *S. palmetto* mortality after 2000, reaching 100% by 2014. *S. palmetto* mortality was 24% by 2014. The rate of mortality of *S. palmetto* in decadent plots was also lower than *J. virginiana*, though, like *J. virginiana*, *S. palmetto* mortality reached 100% by 2014.

3.4 | Understory composition

In 1994, as tidal flooding increased, so did shrubby and herbaceous salt marsh cover, while forest vegetation decreased (Figure 7a). Plots with flooding frequencies of up to 6 weeks in 1994 (including all C

and H plots) supported understory compositions dominated by forest species. Understories of continuous forest plots were dominated by the shrub, *Ilex vomitoria* (yaupon), climbing plants *Smilax bona-nox* (greenbrier) and *Toxicodendron radicans* (poison ivy), and by *Rayjacksonia phyllocephala* (camphor daisy), an annual forb. In healthy island plots, <10% of understory vegetation was composed of salt marsh plants, which included the halophytic shrub, *Lycium carolinianum* (Carolina wolfberry), climbing plant *Ipomoea sagittata* (salt marsh morning glory), and perennial salt marsh grasses *Distichlis spicata* (saltgrass), and *Spartina* spp. (cordgrass). Intermediate island plots supported mixed understories of forest forbs (mainly *R. phyllocephala* and *Solidago* sp. (goldenrod)), halophytic shrubs *L. carolinianum* and *Iva frutescens* (marsh elder), and *D. spicata* and *Spartina* spp. All but two forest species, *R. phyllocephala* and *Solidago* sp., disappeared from decadent plots, which flooded during 17–27 weeks in 1994 and supported *L. carolinianum*, *I. frutescens*, the perennial forb *Borrichia frutescens* (seaside oxeye), and salt marsh grasses.

Between 1994 and 2014, distinct transitions from forest understory to salt marsh shrubs to herbaceous salt marsh had occurred along an increased tidal flooding gradient (Figure 7b). Relative cover of forest species decreased as salt marsh shrubs became dominant in moderately flooded plots and by 2014, herbaceous marsh plants almost exclusively dominated the most frequently flooded plots. As in 1994, plots with flooding frequencies of 0–1 week (continuous forest plots, H0, and H1) maintained understories composed of forest species. In 2014, dominant plants in these plots included *I. vomitoria*, *S. bona-nox*, and two native grasses: *Oplismenus hirtellus* (woodsgrass) and *Dichanthelium dichotomum* (cypress witchgrass). Healthy plots H2 and H3, in which flooding frequency increased from 7 to 13 weeks, supported a combination of forest and salt marsh vegetation. Most common in these plots were perennial upland forbs *Dicliptera sexangularis* (sixangle foldwing) and *Iresine dif-fusa* (Juba's bush), salt marsh shrubs *L. carolinianum* and *I. frutescens*, and annual salt marsh forb *Suaeda linearis* (sea blite). Intermediate plots flooded during approximately 18–20 weeks and were dominated by *L. carolinianum* and *I. frutescens*, perennial salt marsh forbs, including *B. frutescens* and *Batis maritima* (saltwort), and the salt tolerant grass *D. spicata*. Forest vegetation was absent in decadent plots, which flooded during 24–33 weeks in 2014; these plots were dominated by *B. maritima*, *B. frutescens*, and *D. spicata*. Although species composition changed, no difference was found in overall species richness in the 13 plots between 1994 and 2014 ($t = -0.22$, $p = .41$).

We interpreted three-dimensional NMS solutions of plot ordination scores for 1994 and 2014 understory data that were significant according to randomization tests (1994: final minimum stress score = 0.730, $p = .004$; 2014: final minimum stress score = 0.553, $p = .004$). The NMS solution for 1994 compositional data show plots closer together in ordination space than in 2014 (Figure 8a). Plots in the 2–9 weeks tidal flooding category (H2 and H3) in 1994 stretched between plots that received 0–1 week of tidal flooding and plots that received 10 or more weeks of flooding, whereas plots that flooded during 10 or more weeks were clustered tightly together. In 2014,

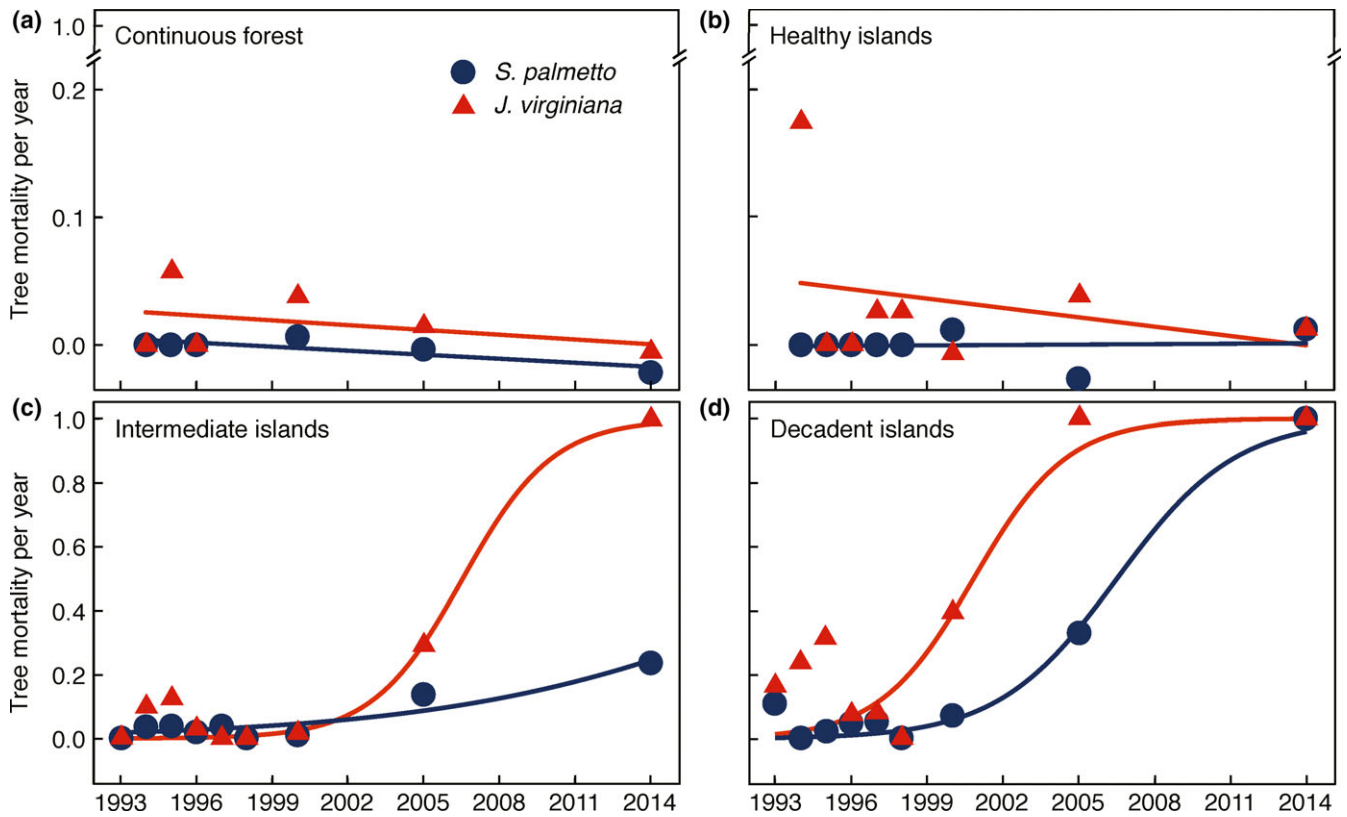


FIGURE 6 Annual mortality rates of *Sabal palmetto* and *Juniperus virginiana* trees; panels (a) and (b) show mortality in the continuous forest plots ($n = 3$) and healthy forest islands ($n = 4$), respectively, from 1993 to 2014 and are fitted with a simple linear model. The y-axes are scaled to make trends more visible. Panels (c) and (d) show mortality in intermediate islands ($n = 3$) and decadent islands ($n = 3$), respectively, from 1992 to 2014 and are fitted with nonlinear logistic growth models

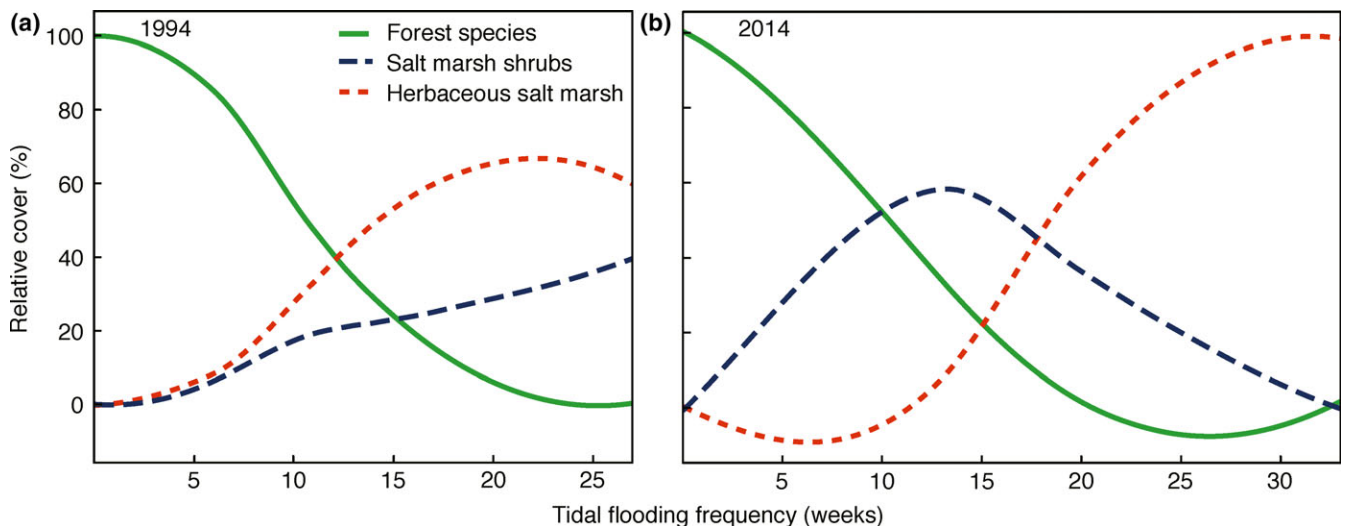


FIGURE 7 Comparison of understory vegetation type (forest species, salt marsh shrubs, and herbaceous salt marsh) between (a) 1994 and (b) 2014 across tidal flooding gradients plotted against that year's tidal flooding frequencies. Increases in 2014 tidal flooding are indicated by an extended x-axis. For clarification, no forest species were present in the most flooded plots in 2014; upswinging tails are artifacts of loess smoothing

plots occupied a wider ordination space and were clustered by tidal flooding group. Plots in the 0–1 week tidal flooding group were farther from the rest of the plots and H1 was shifted closer to the more

frequently flooded stands. Increases in tidal flooding resulted in shifts in tidal flooding groups. Plots H2, H3, and I3 (10–19 weeks flooding group) overlapped slightly with ordination space occupied by plots in

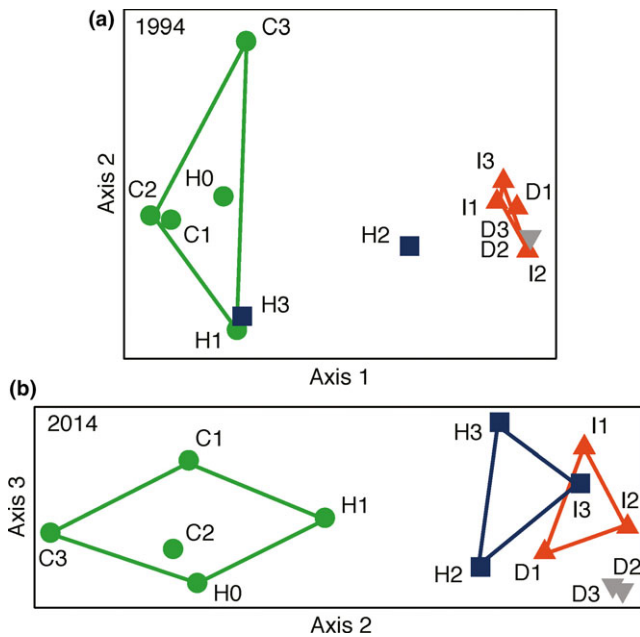


FIGURE 8 NMS solutions with three axes for (a) 1994 and (b) 2014 understory vegetation. Plots are grouped by flooding frequency categories (weeks). 1994: 0–1 (green circles), 2–9 (blue squares), 10–19 (red triangles), and >20 (gray inverted triangles). 2014: 0–1 (green circles), 10–19 (blue squares), 20–29 (red triangles), and >30 (gray inverted triangles)

the 20–29 weeks flooding group. Compared to the 1994 ordinations, these plots occupied a more distinct space between the 10–19 weeks flooding group and >30 weeks flooding group.

4 | DISCUSSION

4.1 | Physical environment dynamics

Spatial variation in tidal flooding frequency represents increased tidal flooding over time as a result of sea level rise. The rate of local mean sea level rise increased from 1.5 mm/year from 1939–1993 to 1.93 mm/year from 1914 to 2014 (NOAA: Center for Operational Oceanographic Products and Services, 2013; Williams, Ewel, et al., 1999), increasing the frequency of flooding on forest islands (Table 1). Tidal flooding in H2 and H3 doubled between 1993 and 2014, and came to match the frequencies in intermediate plots in 1992. Similarly, 2014 flooding frequencies in intermediate plots overlapped the D1 flooding frequency in 1992. While field observations indicate tidal flooding remained infrequent in continuous forest plots and H0 and H1 between 1992 and 2014, we found evidence of flooding in H1 from Hurricane Hermine, a category 1 storm that made landfall north of Turtle Creek in September 2016. Approximately 2–5 cm of wrack (composed mostly of *J. roemerianus*) was deposited on the island containing plot H1.

Frequency of tidal flooding on islands is largely dependent on elevation, which ranged from 0.52 to 0.96 m NAVD (Table 1). Overlap between original field data and 2007 LiDAR data were sufficient

to conclude forest island elevation remained stable over time, which is consistent with regional geology (Castaneda & Putz, 2007; Raabe & Stumpf, 2016; Raabe et al., 2004; Williams, MacDonald, et al., 2007). No relationship between elevation and tidal flooding frequency has been explicitly measured for continuous forest plots (C1, C2, C3), which ranged from 0.69 to 1.10 m NAVD. Continuous forest stands are located farther upstream from the Gulf of Mexico, buffered by surrounding forest, and located farther away from Turtle Creek than the island plots, which all reduce the incidence of tidal flooding.

Lack of correlation between soil depth and elevation or tidal flooding across forest island plots, and large soil depth variations within plots (Figure 2) indicate that a number of interactive physical processes are influencing rates of soil accretion, deposition, organic matter decomposition, and erosion including elevation, tidal flooding frequency, storm events, micro-topography, and vegetation composition. The relatively deep soil in I2 may mean this island receives more sediment from coastal storms than other islands. However, Williams et al. (2003) found forest islands received much less sediment from the 1993 “Storm of the Century” compared to the surrounding marsh. Alternatively, I2 may have more limestone dissolution holes that fill with sediment than the other islands, increasing overall soil depth and micro-topographic variation across the island.

While long-term temperature and precipitation data for our study area suggest that local climate conditions are relatively stable (Figure 3a), freshwater from the Waccasassa River is increasingly unavailable (Figure 3b). Declined flow may be related to the 1998–2002 drought, but the continued negative trend is not explained by reduced precipitation or increased temperatures causing higher regional evapotranspiration. Instead, declining river flow may be indicative of human impacts such as increased water withdrawal upstream and groundwater withdrawal from the regional aquifer (Marella, 2014).

4.2 | Tree survival trends

In the 1980s, causes of *S. palmetto* die off and forest decline were attributed to land-use changes due to agriculture, residential and commercial development, and pine plantations (Vince, Humphrey, & Simons, 1989). Not until the previously published studies on Turtle Creek was sea level rise identified as the primary driver of freshwater forest decline in Waccasassa. Simultaneous loss of *S. palmetto* and expansion of salt marsh vegetation in 2014 in forest islands affirms the loss of forest islands with increased tidal flooding due to sea level rise (Figure 4). Dramatic decreases in species richness in trees, *S. palmetto* regeneration, and *S. palmetto* survival have occurred over a relatively short time period (Figure 5). Forest islands that flooded more than 1 week no longer support any tree regeneration (Table 2) and those that flooded more than 13 weeks no longer support any trees, and have converted to salt marsh. In 2014 two previously healthy island stands (H2 and H3) were more similar to intermediate stands in 1992, and intermediate stands in 2014 were

generally more degraded than even the decadent stands in 1992. These shifts in forest health are consistent with previously noted impacts of salinity on freshwater forest trees along the Big Bend (Doyle, Krauss, Conner, & From, 2010; Liu et al., 2017; Perry & Williams, 1996; Ross, Sah, Meeder, Ruiz, & Telesnicki, 2013; Williams et al., 1998; Williams, Ewel, et al., 1999; Zhai, Jiang, DeAngelis, & Silveira Lobo Sternberg, 2015).

Forest decline was apparent in continuous forest plots even though we observed no evidence of tidal flooding. While *S. palmetto* survival remained high, tree species richness and *S. palmetto* regeneration declined substantially between 1992/1993 and 2014 (Figure 5). One potential explanation is saltwater intrusion. Without a consistent buffering source of freshwater discharge from surface drainage or diffuse groundwater flow, an increase in sea level and tidal flooding along the coastal fringe may increase saltwater intrusion into the shallow aquifer (Kaplan et al., 2010), which could decrease survival of young trees and seedlings in continuous forest stands (Kaplan, Muñoz-Carpena, & Ritter, 2010). Plot C3, which is adjacent to a brackish pond and has a much lower elevation than the other two continuous forest plots, may be most susceptible to potential saltwater intrusion. In addition to having few tree seedlings, its understory lacks the forest shrubs and grasses dominant in C1 and C2 that are typical of coastal freshwater forest. Instead, in 2014 the understory of C3 was dominated by *Cladium jamaicense* (sawgrass), a sedge common in fresh and brackish marshes that can withstand salinities of up to five parts per thousand (Wolfe, Drew, & Handley, 1990), and may signal fresh and saltwater mixing. In 1994, *C. jamaicense* was absent in C3, but was present in high density in plot I1, which indicated potential groundwater flow through the limestone dissolution holes to that forest island (Williams, Ewel, et al., 1999). By 2014, more salt-tolerant species replaced *C. jamaicense* in I1. If, as identified by Williams, Ewel, et al. (1999), declines in tree regeneration is the first major sign of forest die off in otherwise healthy-looking forest stands, we may be witnessing in continuous forest that witnessed decades earlier on forest islands surrounded by salt marsh.

Long-term trends in tree mortality showed *S. palmetto* and *J. virginiana* mortality rates increased with time as forest health continued to decline in intermediate and decadent plots (Figure 6c,d). In contrast, mortality remained low and stable over time in continuous forest and infrequently flooded island stands (Figure 6a,b). Lower salt tolerance partially explains higher mortality of *J. virginiana* than *S. palmetto*, in intermediate and decadent stands. Greater susceptibility to uprooting from the 1993 "Storm of the Century" and water stress (combined with tidal flooding) during the 1998–2002 La Niña drought also spurred *J. virginiana* mortality (DeSantis et al., 2007; Williams et al., 2003). Hurricanes Beryl and Debby and associated storm surges in 2012 may have punctuated tree loss in intermediate and decadent stands since 2005. Salt spray from storms may also have contributed to tree mortality by damaging young trees and new shoots (Wells & Shunk, 1938). In the absence of seedlings, *S. palmetto*, representing the last vestiges of relict freshwater forest, became the last to succumb to the combined effects of tidal flooding, salinity, and severe weather events in decadent plots by 2014.

4.3 | Community reassembly

A historical high rate of change in coastal communities across the Big Bend region illustrates the dynamic and responsive nature of vegetation communities along this relatively undeveloped coastline. Not only is sea level rise driving long-term deterioration of coastal freshwater forest, but it is also driving community reassembly in relict islands. Loss of forest species creates available space in the landscape, providing opportunities for other communities (e.g., shrubby high marsh and herbaceous low marsh) to colonize islands that historically supported freshwater forest. We observed complete turnover in species composition on relict forest islands in response to changing environmental conditions over the course of 20 years (Figure 7). As trees died with increased tidal flooding, they were replaced by salt marsh shrubs, which in turn were replaced by herbaceous salt marsh vegetation at higher tidal flooding frequencies. Replacement of freshwater forest by halophytic communities is just one of many examples of climate change-driven community reassembly (Novak, Moore, & Leidy, 2011; Schaefer, Jetz, & Boehning-Gaese, 2008; Scott & Morgan, 2012) observed in various systems around the world. For example, Beaupre, Edwards, Brander, Luczak, and Ibanez (2008) found species turnover across trophic levels in marine ecosystems of the North Atlantic, a region particularly sensitive to changes in ocean temperature. Schaefer et al. (2008) found that the combined effects of increases in winter and spring temperatures and reduced spring precipitation led to the reassembly of migratory bird communities in Europe. Climate-driven community reassembly was also explored by Hamann and Wang (2006) using a climate model that predicted the replacement of coniferous forest by hardwoods in British Columbia as dominant conifer species lost suitable habitat and hardwood species at their current climate limit expanded their distributions northward.

Species that composed forest, shrub, and herbaceous salt marsh communities remained similar between 1994 and 2014, hence compositions of more flooded stands serve as predictors for the future compositions of less frequently flooded stands in earlier stages of reassembly. However, coastal storms can also initiate shifts in understory composition in forests (Hook, Buford, & Williams, 1991), complicating the turnover pattern driven by tidal flooding. This effect is most apparent in H2 and H3, which suffered severe damage during the 1993 storm (Williams et al., 2003; Williams, MacDonald, et al., 2007). Uprooting of trees in these plots opened up the canopy, which benefited salt marsh shrubs (*L. carolinianum* and *I. frutescens*). Dominance of these shrubs in 2014 accounts for the shifts in ordination space toward intermediate and decadent plots (Figure 8). Storm-induced disturbances also created opportunities for native species that thrive in disturbed sites but are not typical components of freshwater forest understory or salt marsh. By 2014, H2 and H3 supported dense herbaceous understories of the grass *Cenchrus myosuroides* (big sandbur) and perennial forb *I. diffusa*, two common followers of disturbance, which were present in 1994 but at lower densities. As noted in Williams, MacDonald, et al. (2007), both species may reduce tree regeneration via competition and thereby contribute to regeneration failures in these formerly healthy stands.

4.4 | Informing large-scale responses to climate change

Our study provides an in-depth account of the freshwater forest conversion into salt marsh phenomenon that is occurring all along the Big Bend coast. As sea level rise increases tidal flooding and intensifies coastal storms beyond salt tolerance levels of tree seedlings, regeneration ceases, trees die off, and forest vegetation is replaced by halophytic shrubs, which are then replaced by herbaceous salt marsh (Figure 9). This trajectory was consistent among our study plots and reconnaissance observations of remnant forest islands along nearby tidal creeks confirmed this pattern is occurring on a larger scale. This pattern was also documented by Raabe and Stumpf (2016) in their review of historic topographic surveys and imagery of the Big Bend region. They found that 82 km² of coastal freshwater forest and 66 km² of halophytic shrubs and relict trees (“forest-to-marsh transitional habitat”) along 295 km of coastline converted to salt marsh over 120 years (1875–1995). Although much of the freshwater forest along the Big Bend coast is in protected areas and the region is largely undeveloped, most of the property on the landward side is privately owned, which may restrict landward migration of

forest island ecosystems (Doyle et al., 2010; Enwright, Griffith, & Osland, 2016; Geselbracht, Freeman, Birch, Brenner, & Gordon, 2015). Historically, extensive commercial harvesting of *S. palmetto*, *J. virginiana*, *P. taeda*, and hardwoods common in coastal freshwater forests has occurred on private lands along the Big Bend (Williams, MacDonald, et al., 2007). Due to the low topographic relief of the region, large-scale acquisition may be required to accommodate future forest migration and prevent widespread loss of forest islands.

For forest islands with little to no regeneration, conversion into salt marsh is only as far away as the die off of the current generation of trees. While healthier regenerating islands may persist longer, if the rate of sea level rise continues increasing, even healthy stands will be replaced by salt-tolerant communities, potentially within a matter of decades. Forest islands, unique to a small portion of the coastal network of the United States, will completely disappear. Stands of continuous forest may persist for hundreds of years in the absence of direct human impacts or dramatic increases in sea level or extreme weather events. However, as previously noted, low flow in the Waccasassa River and the potential for restricted landward migration threaten forest survival as climate change continues to alter natural coastal conditions.



FIGURE 9 Pattern of community reassembly in coastal freshwater forest along a tidal flooding frequency gradient: (a) many live trees, reduced regeneration, understory of freshwater forest perennials and annuals; (b) reduced regeneration of dominant trees, understory of freshwater forest, salt marsh encroaching on islands; (c) relict islands with few live trees, understory of salt marsh shrubs; (d) relict islands with no live trees, forest converted to herbaceous salt marsh

Looking beyond the loss of forest islands, future research should evaluate other possible community reassembly trajectories in relict forest islands and changes in ecological functions provided by the Big Bend coast. For example, increasing temperatures and fewer freeze events are driving the expansion of mangrove populations northward along the east and west coasts of Florida (Cavanaugh et al., 2014; Osland, Day et al., 2017; Osland, Feher et al., 2017). Replacement of coastal freshwater forest by *Avicennia germinans* (black mangrove) is already predicted along the southern Gulf Coast of Florida and in the Everglades (Doyle et al., 2010; Ross et al., 2013) and the potential exists for *A. germinans* to become more prominent along the Big Bend. *Avicennia germinans* seedlings are present at the study site and we have found that relict forest islands and surrounding salt marsh can support *A. germinans* establishment, though top-down biotic controls limit colonization (Langston, Kaplan, & Angelini, 2017). Another alternative that must be considered is the northward spread of *Schinus terebinthifolia* (Brazilian pepper) in coastal forests in Florida in response to sea level rise and warming temperatures. *Schinus terebinthifolia* has been reported on two of the 10 islands we studied and is actively treated by park staff. Due to many highly adaptable physical, reproductive, physiological, and genetic characteristics, its potential for widespread invasion along the Big Bend presents an alarming consequence of climate change (Spector & Putz, 2006; Williams, Muchugu, Overholt, & Cuda, 2007). The extent to which different communities replace forest islands largely depends on how these communities respond to continued environmental changes resulting from climate change. We expect reassembly trajectories in relict forest islands will be dictated by local impacts from sea level rise, coastal storms, changing weather regimes, and temperature shifts that will continue to drive short- and long-term ecological changes in the region.

ACKNOWLEDGEMENTS

We thank Waccasassa Bay Preserve State Park for permitting research, University of Florida Seahorse Key Marine Lab for airboat transportation, K. Williams for providing insights and plot data, and G. Christensen, M. D'Angelo, J. Guarin, A. Johnson, E. Labandera, C. Mekwinski, T. Murphy, K. Reaver, N. Reaver, S. Taylor, and D. Walshaw for much appreciated field assistance.

REFERENCES

- Abbott, J. R., & Judd, W. S. (2000). Floristic inventory of the Waccasassa Bay State Preserve, Levy County, Florida. *Rhodora*, *102*, 439–513.
- Angelini, C., & Silliman, B. R. (2012). Patch size-dependent community recovery after massive disturbance. *Ecology*, *93*, 101–110.
- Beaugrand, G., Edwards, M., Brander, K., Luczak, C., & Ibanez, F. (2008). Causes and projections of abrupt climate-driven ecosystem shifts in the North Atlantic. *Ecology Letters*, *11*, 1157–1168.
- Castaneda, H., & Putz, F. (2007). Predicting sea-level rise effects on a nature preserve on the Gulf Coast of Florida: a landscape perspective. *Florida Scientist*, *70*, 166–175.
- Cavanaugh, K. C., Kellner, J. R., Forde, A. J., Gruner, D. S., Parker, J. D., Rodriguez, W., & Feller, I. C. (2014). Poleward expansion of mangroves is a threshold response to decreased frequency of extreme cold events. *Proceedings of the National Academy of Sciences*, *111*, 723–727.
- Cormier, N., Krauss, K. W., & Conner, W. H. (2013). Periodicity in stem growth and litterfall in tidal freshwater forested wetlands: Influence of salinity and drought on nitrogen recycling. *Estuaries and Coasts*, *36*, 533–546.
- Craft, C., Clough, J., Ehman, J., Joye, S., Park, R., Pennings, S., ... Machmuller, M. (2009). Forecasting the effects of accelerated sea-level rise on tidal marsh ecosystem services. *Frontiers in Ecology and the Environment*, *7*, 73–78.
- DeSantis, L. R., Bhotika, S., Williams, K., & Putz, F. E. (2007). Sea-level rise and drought interactions accelerate forest decline on the Gulf Coast of Florida, USA. *Global Change Biology*, *13*, 2349–2360.
- Doyle, T. W., Krauss, K. W., Conner, W. H., & From, A. S. (2010). Predicting the retreat and migration of tidal forests along the northern Gulf of Mexico under sea-level rise. *Forest Ecology and Management*, *259*, 770–777.
- Enwright, N. M., Griffith, K. T., & Osland, M. J. (2016). Barriers to and opportunities for landward migration of coastal wetlands with sea-level rise. *Frontiers in Ecology and the Environment*, *14*, 307–316.
- Fagherazzi, S., Kirwan, M. L., Mudd, S. M., Guntenspergen, G. R., Temmerman, S., D'Alpaos, A., ... Clough, J. (2012). Numerical models of salt marsh evolution: Ecological, geomorphic, and climatic factors. *Reviews of Geophysics*, *50*, RG1002.
- FCC: Florida Climate Center. (2014). *Average annual precipitation*. Center for Ocean-Atmospheric Prediction Studies, Florida State University (climatecenter.fsu.edu/products-services/data/weather-planner-maps/average-annual-precipitation).
- Gabler, C. A., Osland, M. J., Grace, J. B., Stagg, C. L., Day, R. H., Hartley, S. B., ... McLeod, J. L. (2017). Macroclimatic change expected to transform coastal wetland ecosystems this century. *Nature Climate Change*, *7*, 142–147.
- Geselbracht, L. L., Freeman, K., Birch, A. P., Brenner, J., & Gordon, D. R. (2015). Modeled sea level rise impacts on coastal ecosystems at six major estuaries on Florida's gulf coast: Implications for adaptation planning. *PLoS ONE*, *10*, e0132079.
- Geselbracht, L., Freeman, K., Kelly, E., Gordon, D. R., & Putz, F. E. (2011). Retrospective and prospective model simulations of sea level rise impacts on Gulf of Mexico coastal marshes and forests in Waccasassa Bay, Florida. *Climatic Change*, *107*, 35–57.
- Goodbred, S. L., & Hine, A. C. (1995). Coastal storm deposition: Salt-marsh response to a severe extratropical storm, March 1993, west-central Florida. *Geology*, *23*, 679–682.
- Hamann, A., & Wang, T. (2006). Potential effects of climate change on ecosystem and tree species distribution in British Columbia. *Ecology*, *87*, 2773–2786.
- Hook, D. D., Buford, M. A., & Williams, T. M. (1991). Impact of Hurricane Hugo on the South Carolina coastal plain forest. *Journal of Coastal Research*, *8*, 291–300.
- Kaplan, D., Muñoz-Carpena, R., & Ritter, A. (2010). Untangling complex shallow groundwater dynamics in the floodplain wetlands of a southeastern US coastal river. *Water Resources Research*, *46*, <https://doi.org/10.1029/2009WR009038>
- Kaplan, D., Muñoz-Carpena, R., Wan, Y., Hedgepeth, M., Zheng, F., Roberts, R., & Rossmanith, R. (2010). Linking river, floodplain, and vadose zone hydrology to improve restoration of a coastal river affected by saltwater intrusion. *Journal of Environmental Quality*, *39*, 1570–1584.
- Kelly, A. E., & Goulden, M. L. (2008). Rapid shifts in plant distribution with recent climate change. *Proceedings of the National Academy of Sciences*, *105*, 11823–11826.
- Kimberlain, T. B. (2012). *Tropical cyclone report: Tropical storm debby (AL042012) 23–27 June 2012*. Miami, FL: NOAA National Hurricane Center, pp. 1–51.

- Kirwan, M. L., Guntenspergen, G. R., & Morris, J. T. (2009). Latitudinal trends in *Spartina alterniflora* productivity and the response of coastal marshes to global change. *Global Change Biology*, 15, 1982–1989.
- Kirwan, M. L., & Megonigal, J. P. (2013). Tidal wetland stability in the face of human impacts and sea-level rise. *Nature*, 504, 53–60.
- Kurz, H., & Wagner, K. A. (1957). Tidal marshes of the Gulf and Atlantic coasts of northern Florida and Charleston, South Carolina. Florida State University, Studies No. 24, 168.
- Langston, A., Kaplan, D., & Angelini, C. (2017). Predation restricts black mangrove (*Avicennia germinans*) colonization at its northern range limit along Florida's Gulf Coast. *Hydrobiologia*, <https://doi.org/10.1007/s10750-017-3197-0>
- Leffler, A. J., Klein, E. S., Oberbauer, S. F., & Welker, J. M. (2016). Coupled long-term summer warming and deeper snow alters species composition and stimulates gross primary productivity in tussock tundra. *Oecologia*, 181, 287–297.
- Leonardi, N., Ganju, N. K., & Fagherazzi, S. (2016). A linear relationship between wave power and erosion determines salt-marsh resilience to violent storms and hurricanes. *Proceedings of the National Academy of Sciences*, 113, 64–68.
- Lin, N., Emanuel, K., Oppenheimer, M., & Vanmarcke, E. (2012). Physically based assessment of hurricane surge threat under climate change. *Nature Climate Change*, 2, 462–467.
- Liu, X., Conner, W. H., Song, B., & Jayakaran, A. D. (2017). Forest composition and growth in a freshwater forested wetland community across a salinity gradient in South Carolina, USA. *Forest Ecology and Management*, 389, 211–219.
- Marella, R. L. (2014). Water withdrawals, use, and trends in Florida, 2010. Scientific Investigations Report, Reston, VA, 72 pp.
- Mattson, R. A., Frazer, T. K., Hale, J., Blitch, S., & Ahijevych, L. (2007). Florida big bend. In L. Handley, D. Altsman & R. DeMay (Eds.), *Seagrass status and trends in the northern Gulf of Mexico: 1940–2002* (pp. 171–188). Reston, VA: U.S. Geological Survey Scientific Investigations Report 2006-5287 and U.S. Environmental Protection Agency 855-R-04-003.
- Mendelsohn, R., Emanuel, K., Chonabayashi, S., & Bakkenen, L. (2012). The impact of climate change on global tropical cyclone damage. *Nature Climate Change*, 2, 205–209.
- Michener, W. K., Blood, E. R., Bildstein, K. L., Brinson, M. M., & Gardner, L. R. (1997). Climate change, hurricanes and tropical storms, and rising sea level in coastal wetlands. *Ecological Applications*, 7, 770–801.
- NOAA: Center for Operational Oceanographic Products and Services. (2013). Tides & currents: Mean sea level trend 8727520 Cedar Key, Florida, October 15, 2013. http://tidesandcurrents.noaa.gov/sltrends/sltrends_station.shtml?stnid=8727520.
- NOAA: Climate Prediction Center. (2015). Cold and warm episodes by season 1950–2015. National Weather Service, November 4, 2015. http://cpc.ncep.noaa.gov/products/analysis_monitoring/ensostuff/ensoyears.shtml.
- NOAA: National Centers for Environmental Information. (2016). State of the climate: Global analysis for annual 2015. National Climatic Data Center, January 2016. <http://ncdc.noaa.gov/sotc/global/201513>.
- Novak, M., Moore, J. W., & Leidy, R. A. (2011). Nestedness patterns and the dual nature of community reassembly in California streams: A multivariate permutation-based approach. *Global Change Biology*, 17, 3714–3723.
- Osland, M. J., Day, R. H., Hall, C. T., Brumfield, M. D., Dugas, J. L., & Jones, W. R. (2017). Mangrove expansion and contraction at a poleward range limit: Climate extremes and land-ocean temperature gradients. *Ecology*, 98, 125–127.
- Osland, M. J., Enwright, N. M., Day, R. H., Gabler, C. A., Stagg, C. L., & Grace, J. B. (2016). Beyond just sea-level rise: Considering macroclimatic drivers within coastal wetland vulnerability assessments to climate change. *Global Change Biology*, 22, 11.
- Osland, M. J., Feher, L. C., Griffith, K. T., Cavanaugh, K. C., Enwright, N. M., Day, R. H., ... Rogers, K. (2017). Climatic controls on the global distribution, abundance, and species richness of mangrove forests. *Ecological Monographs*, <https://doi.org/10.1002/ecm.1248>
- Peck, J. E. (2010). *Multivariate analysis for community ecologists: Step-by-step using PC-ORD*. Glendon Beach, OR: MjM Software Design.
- Perry, L., & Williams, K. (1996). Effects of salinity and flooding on seedlings of cabbage palm (*Sabal palmetto*). *Oecologia*, 105, 428–434.
- R Core Team. (2016). *R: A language and environment for statistical computing*. Vienna, Austria: <http://www.R-project.org>.
- Raabe, E.A., Streck, A.E., & Stumpf, R.P. (2004). *Historic topographic sheets to satellite imagery: A methodology for evaluating coastal change in Florida's Big Bend tidal marsh*. US Geological Survey, Center for Coastal and Regional Marine Studies. Open-file Report 2002-211.
- Raabe, E. A., & Stumpf, R. P. (2016). Expansion of tidal marsh in response to sea-level rise: Gulf Coast of Florida, USA. *Estuaries and Coasts*, 39, 145–157.
- Reed, D. J. (1995). The response of coastal marshes to sea-level rise: Survival or submergence? *Earth Surface Processes and Landforms*, 20, 39–48.
- Ross, M. S., Sah, J. P., Meeder, J. F., Ruiz, P. L., & Telesnicki, G. (2013). Compositional effects of sea-level rise in a patchy landscape: The dynamics of tree islands in the southeastern coastal Everglades. *Wetlands*, 34, 91–100.
- Scavia, D., Field, J. C., Boesch, D. F., Buddemeier, R. W., Burkett, V., Cayan, D. R., ... Mason, C. (2002). Climate change impacts on US coastal and marine ecosystems. *Estuaries*, 25, 149–164.
- Schaefer, H.-C., Jetz, W., & Boehning-Gaese, K. (2008). Impact of climate change on migratory birds: Community reassembly versus adaptation. *Global Ecology and Biogeography*, 17, 38–49.
- Scott, A. J., & Morgan, J. W. (2012). Early life-history stages drive community reassembly in Australian old-fields. *Journal of Vegetation Science*, 23, 721–731.
- Sheil, D., Burslem, D. F., & Alder, D. (1995). The interpretation and misinterpretation of mortality rate measures. *Journal of Ecology*, 83, 331–333.
- Spector, T., & Putz, F. E. (2006). Biomechanical plasticity facilitates invasion of maritime forests in the southern USA by Brazilian pepper (*Schinus terebinthifolius*). *Biological Invasions*, 8, 255–260.
- Svenning, J.-C., & Sandel, B. (2013). Disequilibrium vegetation dynamics under future climate change. *American Journal of Botany*, 100, 1266–1286.
- USGS. (2012). *NWIS site information for USA: Site inventory 02313700 Waccasassa River NR Gulf Hammock, FLA*. http://waterdata.usgs.gov/nwis/inventory/?site_no=02313700&agency_cd=USGS.
- Verdi, R.J., Tomlinson, S.A., & Marella, R.L. (2006). *The drought of 1998–2002: Impacts on Florida's hydrology and landscape*. US Geological Survey. Circular 1295.
- Vince, S. W., Humphrey, S. R., & Simons, R. W. (1989). *The ecology of hydric hammocks: A community profile*. Washington, DC: US Fish and Wildlife Service, Gainesville, FL: Florida Museum of Natural History, 95 pp.
- Walther, G. R., Post, E., Convey, P., Menzel, A., Parmesan, C., Beebee, T. J. C., ... Bairlein, F. (2002). Ecological responses to recent climate change. *Nature*, 416, 389–395.
- Wells, B. W., & Shunk, I. V. (1938). Salt spray: An important factor in coastal ecology. *Bulletin of the Torrey Botanical Club*, 65, 485–492.
- White, E., & Kaplan, D. (2017). Restore or retreat? Saltwater intrusion and water management in coastal wetlands. *Ecosystem Health and Sustainability*, 3, <https://doi.org/10.1002/ehs1002.1258>
- Williams, K., Ewel, K. C., Stumpf, R. P., Putz, F. E., & Workman, T. W. (1999). Sea-level rise and coastal forest retreat on the west coast of Florida, USA. *Ecology*, 80, 2045–2063.
- Williams, K., MacDonald, M., McPherson, K., & Mirti, T. H. (2007). Chapter 10: Ecology of the Coastal Edge of hydric hammocks on the Gulf Coast of Florida. In W. Conner, T. Doyle, & K. Krauss (Eds.), *Ecology of tidal freshwater forested wetlands of the southeastern United States* (pp. 255–289). Netherlands: Springer.

- Williams, K., MacDonald, M., & Sternberg, L. D. S. L. (2003). Interactions of storm, drought, and sea-level rise on coastal forest: A case study. *Journal of Coastal Research*, *19*, 1116–1121.
- Williams, K., Meads, M. V., & Sauerbrey, D. A. (1998). The roles of seedling salt tolerance and resprouting in forest zonation on the west coast of Florida, USA. *American Journal of Botany*, *85*, 1745–1752.
- Williams, D., Muchugu, E., Overholt, W., & Cuda, J. (2007). Colonization patterns of the invasive Brazilian peppertree, *Schinus terebinthifolius*, in Florida. *Heredity*, *98*, 284–293.
- Williams, K., Pinzon, Z. S., Stumpf, R. P., & Raabe, E. A. (1999). *Sea-level rise and coastal forests on the Gulf of Mexico*. US Geological Survey. Open-file Report 99-441.
- Wolfe, S. H., Drew, R. D., & Handley, L. (1990). *Ecological characterization of the Tampa Bay watershed*. Tallahassee, FL: US Fish and Wildlife Service Biological Report, 20 pp.
- Zhai, L., Jiang, J., DeAngelis, D., & Silveira Lobo Sternberg, L. (2015). Prediction of plant vulnerability to salinity increase in a coastal ecosystem by stable isotope composition ($\delta^{18}O$) of plant stem water: A model study. *Ecosystems*, *19*, 32–49.

How to cite this article: Langston AK, Kaplan DA, Putz FE. A casualty of climate change? Loss of freshwater forest islands on Florida's Gulf Coast. *Glob Change Biol*. 2017;00:1–14. <https://doi.org/10.1111/gcb.13805>